Correspondence: Jianghua Sun, State Key Laboratory of Integrated Management of Pest Insects and Rodents, Institute of Zoology, Chinese Academy of Sciences, Beijing 100101, China. Tel: +86 10 64807121; fax: +86 10 64807099; email: sunjh@ioz.ac.cn

ORIGINAL ARTICLE

A new bacteria-free strategy induced by MaGal2 facilitates pinewood nematode escape immune response from its vector beetle

Chi Zhang[1.2], Jacob D. Wickham[1], Lilin Zhao[1.2] and Jianghua Sun[1.2]

[1]*State Key Laboratory of Integrated Management of Pest Insects and Rodents, Institute of Zoology, Chinese Academy of Sciences, Beijing 100101, China;*

[2]*CAS Center for Excellence in Biotic Interactions, University of Chinese Academy of Sciences, Beijing 100049, China*

This is an Accepted Article that has been peer-reviewed and approved for publication in the Insect Science but has yet to undergo copy-editing and proof correction. Please cite this article as doi: 10.1111/1744-7917.12823.

Abstract

Symbiotic microbes play a crucial role in regulating parasite–host interactions; however, the role of bacterial associates in parasite–host interactions requires elucidation. In this study, we showed that, instead of introducing numerous symbiotic bacteria, dispersal of fourth-stage juvenile (J_{IV}) pinewood nematodes (PWNs), *Bursaphelenchus xylophilus*, only introduced few bacteria to its vector beetle, *Monochamus alternatus* (*Ma*). J_{IV} showed weak binding ability to five dominant bacteria species isolated from the beetles' pupal chamber. This was especially the case for binding to the opportunistic pathogenic species *Serratia marcescens*; the nematodes' bacteria binding ability at this critical stage when it infiltrates *Ma* for dispersal was much weaker compared with *Caenorhabditis elegans*, *Diplogasteroides asiaticus*, and propagative-stage PWN. The associated bacterium *S. marcescens*, which was isolated from the beetles' pupal chambers, was unfavorable to *Ma*, because it caused a higher mortality rate upon injection into tracheae. In addition, *S. marcescens* in the tracheae caused more immune effector disorders compared with PWN alone. Ma_Galectin2 (MaGal2), a pattern-recognition receptor, was up-regulated following PWN loading. Recombinant MaGal2 protein formed aggregates with five dominant associated bacteria *in vitro*. Moreover, MaGal2 knockdown beetles had up-regulated prophenoloxidase gene expression, increased phenoloxidase activity, and decreased PWN loading. Our study

revealed a previously unknown strategy for immune evasion of this plant pathogen inside its vector, and provides novel insights into the role of bacteria in parasite–host interactions.

Key words galectin; immune evasion; pinewood nematode; symbiotic bacteria; vector beetle

Introduction

Microbes play vital roles in regulating various aspects of host physiology, such as development, immune regulation, defense, and nutrition (Backhed *et al.*, 2005; Zhang *et al.*, 2018b; Wu *et al.*, 2019a). In insects, symbiotic microbes colonize most tissues, including the exoskeleton and gut, and even occur within insect cells (Douglas, 2015; Lu *et al.*, 2016). The insect host can benefit from symbiotic interactions with microbes, and the microbes benefit from being spread by the host and having a location to reproduce (Douglas *et al.*, 2001; Nakanishi *et al.*, 2008; Morales-Jimenez *et al.*, 2009).

Although some microbes are symbiotic, many are pathogenic, and the host needs to be able to sufficiently distinguish these types of microbes. The innate immune system plays a crucial role in detecting and eliminating potential microbial pathogens in most metazoans (Brubaker *et al.*, 2015). In arthropods, melanization is the earliest response triggered by invaders. This pathway includes the cleavage of prophenoloxidase (PPO) to phenoloxidase

(PO), and active PO contributes to killing bacteria, fungi, and pathogenic nematodes, and results in the black pigment melanin being deposited at the wound site and around the invader's body (Yuan *et al.*, 2017; Cheng *et al.*, 2018b).

In symbiotic relationships, the host maintains symbiosis with specific microorganisms by its immune system evolving, and bacteria can change their surface molecules, such as proteins or other markers, to facilitate coexistence (Belkaid & Harrison, 2017). Symbiotic bacteria could also help pathogenic nematodes resist host defenses. In contrast, susceptible nematodes are eliminated by an array of host immune responses, including the PO cascade, antimicrobial peptides (AMPs), and reactive oxygen species (ROS) (Ji & Kim, 2004; Park *et al.*, 2004; Castillo *et al.*, 2011; Binda-Rossetti *et al.*, 2016; Sadekuzzaman *et al.*, 2017). Moreover, galectins serve as pattern-recognition receptors (PRRs), which function in pathogen detection and trigger subsequent innate immune responses, including humoral and cellular immune responses (Tanji & Ip, 2005; Vasta, 2009; Kurata, 2010; Castillo *et al.*, 2011).

The pinewood nematode (PWN), *Bursaphelenchus xylophilus*, which is the causative agent of pine wilt disease (PWD), is vectored by pine sawyer beetles, *Monochamus alternatus*, and threatens the safety and stability of pine forest ecosystems (Zhao *et al.*, 2013; Zhao *et al.*, 2014). Unlike the free-living nematode model species *Caenorhabditis elegans*, PWN have two distinct life stages (dispersive and propagative). To complete its life

cycle, each stage requires a unique host relationship, which range from symbiotic/commensal (with *Monochamus* beetles) to parasitic (with pine trees).

Previous studies showed that third-stage juveniles were attracted by specific categories of terpenes produced by mature insect larvae and aggregated around the pupal chamber in diseased trees (Zhao *et al.*, 2007). Fourth-stage juveniles (J_{IV}) of PWN, of which there are several hundred up to as many as 200 000 per beetle, enter the tracheal system of the newly eclosed beetle for dispersal, where they remain in the tracheal system for up to 1 month (Fielding & Evans, 1996). Then, PWNs are carried by newly eclosed beetles and dispersed to healthy pine trees for subsequent maturation feeding. The elevated bursts of CO_2 that result from increased beetle activity triggers the nematodes' departure from their spiracles, and they enter the healthy pine trees via feeding wounds on pine branches (Wu *et al.*, 2019b). Recently, some studies reported that associated bacteria and fungi also contribute to the pathogenicity of PWN (Nascimento *et al.*, 2015; Proenca *et al.*, 2017). However, how the potential microbial associates of PWN or even PWN itself escape the immune response of the beetle remains unknown.

A previous study reported the immune interactions between the PWN and its insect vector *M. alternatus*, and revealed that PWNs induce production of epithelial ROS in vector beetles, whereas up-regulation of antioxidative genes balanced the ROS level in the tracheal system (Zhou *et al.*, 2018). Moreover, melanization and some AMPs showed no significant

changes in the tracheae when loaded with PWNs, although some serine protease inhibitors were activated in vector beetles carrying PWNs (Zhou *et al.*, 2018). However, the exact role played by the PWN-transferred bacteria in the immune modulation of the host vector remains unknown.

In this study, we showed that J_{IV} nematodes carry relatively few bacteria from the pupal chamber into the tracheal system and therefore prevent balance disruption of the immune system. The bacteria carrying ability in J_{IV} was weaker compared with that of other nematode species. Furthermore, the bacterial species *Serratia marcescens*, isolated from pupal chambers, is pathogenic to vector beetles when either introduced alone or co-inoculated with PWNs in the tracheae. Moreover, the expression level of MaGal2, a PRR that recognizes bacteria and fungi, was significantly up-regulated in both tracheal and epidermal tissues loaded with PWN. RNAi depletion of MaGal2 significantly decreased the amount of PWN loading, whereas the PO activity increased. Taken together, these findings revealed a previously unknown strategy for immune evasion of this plant pathogen inside its vector that involves the immune response mediator MaGal2, which likely contributes to the stability of the symbiotic relationship between PWNs and vector beetles; this enables its fast and widespread invasion dynamics, and ultimately causes devastating damage to pine forests worldwide.

Materials and methods

Experimental organisms

Monochamus alternatus were maintained in the laboratory for over 10 generations and reared on artificial diet at 26 ± 1°C under a photoperiod of 14 h/10 h (light/dark). Late-stage pupae and newly eclosed adults, reared in darkness, were used in experiments. PWNs were selected from a colony maintained in laboratory conditions for more than 5 years at 26 ± 1°C in darkness.

Bacteria, which included *S. marcescens, Pseudomonas* sp., *Flexibacter aurantiacus*, *Pantoea* sp., and *Curtobacterium oceanosedimentum*, were isolated and molecularly identified with 16s rDNA from dead pine trees in Jiangsu and Zhejiang provinces, China.

Caenorhabditis elegans wild-type N2 nematodes were maintained at 20°C, as previously described (Brenner, 1974). *Diplogasteroides asiaticus* were separated from samples of dead pine trees sourced from Shaanxi and Anhui provinces using the Baermann funnel method and identified as previously described by Zhou *et al.* (2018).

Bacteria quantity in tracheae

To obtain *Monochamus* beetles carrying PWN, artificial barley medium (ABM) was used as previously described (Zhou *et al.*, 2018). Briefly, 10 g barley seed and 15 mL distilled water were autoclaved at 121°C for 30 min in a 50-mL conical flask; then, *Botrytis cinerea* was inoculated as food for PWNs and cultured for 10 days at 25°C, after which approximately 1000 propagative-stage PWNs were added to the medium. Early-stage pupae were added to medium 10 days after the PWNs were added, and sawdust was added to prevent overexposing the beetles to moisture and contact with the medium. *Monochamus* beetles not carrying PWN were reared in sawdust. At 5 days after eclosion, beetles were dissected and the tracheae were carefully excised.

For the spread plate method, tracheae were placed in a 1.5-mL sterile tube with 100 μL sterile phosphate buffer saline (PBS) buffer, and then homogenated and diluted with PBS buffer for spreading. Exactly 100 μL of diluted homogenate were spread on tryptic soy agar (TSA) medium plates and cultured at 25°C for 5 days. A 1 : 100 dilution was used based on the amount and density of colony-forming units (CFUs). Plates were photographed with a digital camera.

For relative quantity determination, tracheae were placed in a 1.5-mL sterile tube with 100 μL with MightyPrep reagent for DNA (Takara, Japan) and homogenated; then, the

homogenate was incubated at 95°C for 10 min followed by centrifugation at 13000 *g* for 3 min. The supernatant was collected as template for real-time quantitative PCR (RT-qPCR), as previously described (Wei *et al.*, 2017b).

Bacteria carrying ability assay of PWNs in vivo

ABM was prepared as previously described. Relative to controls, 100 μL *S. marcescens* cultured in tryptic soy broth (TSB) medium was added 1 week after PWN addition. The early-stage pupae were placed in medium 10 days after PWN addition, and sawdust was added to prevent direct contact between bacteria and beetles. At 5 days after eclosion, the beetle was dissected and the bacteria were detected by spread plate method, as previously described. Plates were cultured for 3 days at 25°C.

Evaluation of bacteria binding to nematodes

The bacteria were grown on a TSA plate and coated on a new plate to form bacteria circles with empty middles and a thin edge of bacteria around the perimeter (approximately 6 mm in diameter) (Fig. S1A). Subsequently, one nematode was transferred using a pipette

to the center of the bacteria circle and allowed to creep out of the circle to ensure sufficient contact with bacteria (Fig. S1B); the nematode was then immediately pipetted out with a small aliquot (0.5 μL) of TSB medium and transferred to 200 μL TSB medium. The nematode-containing TSB medium was ultrasonicated and vortexed for 30 s, and 100 μL from the remaining volume was spread on a TSA plate and cultured at 25°C for 16–48 h, as per the requirements of each bacteria species. The bacteria that bound to the nematode were determined by counting CFUs.

Insect infection and survival rate analysis

Newly eclosed (2 days after eclosion) adult beetles were used for infection studies. *Serratia marcescens* were cultured at a final concentration of OD_{600} = 0.5. One milliliter was collected following centrifugation for 1 min at 13000 *g*. The supernatant was discarded and bacteria were resuspended in 1 mL sterile water. Following a 10-fold dilution in sterile water, 0.5 μL of 10^4 CFUs were added to each beetle trachea, and tissue samples were collected 24 h post-infection. A total of 20 beetles were used in each group, and samples were collected from surviving beetles. Three replicates were included for each experiment. For survival rate analysis, at least 10 beetles were used for each group. The Kaplan–Meier survival analysis was performed using GraphPad Prism version 7.0 for Windows (GraphPad

Software, La Jolla, California, USA, www.graphpad.com). Log-rank (Mantel Cox test) was used to calculate statistical significance.

RNA sample preparation, cDNA synthesis, and RT-qPCR analysis

The tracheae and epidermises of adult beetles were collected and frozen in liquid nitrogen for RNA isolation. Trizol Reagent (Invitrogen, Carlsbad CA, USA) was used for total RNA extraction. One microgram of total RNA was used in each cDNA synthesis reaction using the FastQuant RT kit (Tiangen, Beijing, China) according to the manufacturer's instructions. RT-qPCR was performed on an ABI 7300plus system using the SYBR premix ExTaq (Tiangen, Beijing, China) with specifically designed primers. The $2^{-\Delta\Delta Ct}$ method was used to calculate relative mRNA expression level, and *β*-actin was used as an internal control. Results were shown as mean ± SEM of three independent biological replicates. Student's *t*-test was used to calculate statistical significance at the $\alpha = 0.05$ level.

PO activity assay

Tracheal and epidermal tissues were collected from adult beetles and then homogenized with PBS (pH = 7.5), followed by centrifugation at 8000 *g* for 10 min at 4 °C.

The resulting supernate was pipetted into a new tube. After incubation at 25°C for 2 h, 50 μL supernate was added to 200 μL substrate solution [2 mmol/L dopamine in 50 mmol/L sodium phosphate buffer (pH = 6.5)]. Protein concentration was determined with a BCA Protein Assay kit (CWbio, Beijing, China) according to the manufacturer's instructions. PO activity was determined at 470 nm using a microplate reader, and each sample was performed in triplicate wells. One unit of activity was defined as ΔA470 of 0.001 in 1 min using 50 μg of protein.

Heatmap analysis

Heatmap analysis was performed by using R package "pheatmap" (http://www.r-project.org/; R Foundation for Statistical Computing,Wien, Austria) as described by Zhou *et al.* (2018). Previous published data by Zhou *et al.* (2018) was used for heatmap analysis.

MaGal2 cloning and structure prediction

Based on the transcript data, a MaGal2 gene with a 1209-bp open reading forum (ORF) was annotated. Then, the MaGal2 gene was cloned with specific primers, and the isoforms

were sequenced and analyzed using blast in NCBI (https://www.ncbi.nlm.nih.gov/). The protein structure was predicted in swiss-model (https://swissmodel.expasy.org/) with full-length protein sequence.

Protein expression and polyclonal antibody preparation

The MaGal2 ORF was amplified from cDNA of adult epidermis using Phusion® High-Fidelity DNA Polymerase (New England BioLabs, Ipswich, MA, USA), and then cloned into the pET28a vector. The recombinant MaGal2 was induced by 0.5 mmol/L Isopropyl b-D-1-Thiogalactopyranoside (Sigma Aldrich, St. Louis, MO, USA) and purified using Ni-NTA superflow (Qiagen, Hilden, Germany). The soluble protein concentration was measured as mentioned above and then stored in −80°C for later use. The polyclonal antibody against MaGal2 was produced using recombinant protein by immunizing rabbits (Beijing Protein Innovation, Beijing, China).

Immunoblot analysis

Tissues were homogenized with RIPA lysis buffer and then centrifuged at 13 000 *g* for 10 min at 4 °C. Protein samples were collected from the supernatant, resolved on 4%–15% gradient sodium dodecyl sulfate–polyacrylamide gel electrophoresis (SDS–PAGE) (Bio-Rad Laboratories, Hercules, CA, USA), and electrotransferred to polyvinylidene difluoride (PVDF) membranes (Thermo Fisher Scientific, Inc., Waltham, MA, USA). Following membrane blocking, the membranes were incubated with the primary polypeptide antibody against MaGal2 (dilution 1 : 5000) overnight at 4°C. α-Tubulin (11H10) rabbit mAbs (Cell Signaling Technology, Danvers, MA, USA) was used as the loading control. The secondary antibody [dilution 1:10,000; goat anti-rabbit IgG (H + L) HRP conjugate; Promega, Madison, WI, USA] was then applied for 2 h, followed by visualization with a SuperSignal West Pico substrate (Pierce Biotechnology, Appleton, WI, USA).

Agglutination and binding analysis of MaGal2

For the agglutination assay, suspension of five bacterial isolates from the field were incubated with recombinant soluble MaGal2 for 3 h (500 μg/mL), as previously described (Yu & Kanost, 2000, Dawadi *et al.*, 2018), and bovine serum albumin (Bio-Rad, Hercules, CA,

USA) was used as a negative control. Samples were transferred to glass slides and images were acquired with a BX51 microscope (Olympus, Tokyo, Japan). In addition, two fluorescence-labeled microbes, fluorescein conjugate Zymosan (Invitrogen) and Alexa Fluor™ 594 conjugate *Staphylococcus aureus* (Invitrogen), were treated as above, and images were acquired with a Zeiss LSM 710 confocal microscope (Carl Zeiss Microscopy GmbH, Jena, Germany).

Synthesis and microinjection of dsRNA to test PWN loading

Double-stranded RNAs (dsRNAs) were synthesized as previously described (Volovych *et al.*, 2019; Wang *et al.*, 2019). Briefly, the sense and antisense primers were designed to generate cDNA fragments of MaGal2 by PCR. The T7 RiboMAX Express RNAi kit (Promega) was used to synthesize dsRNA, and the green fluorescent protein (GFP) gene was used as control dsRNA (dsGFP). Approximately 30 μg of each dsRNA was injected into the hemocoel of each Late-stage pupa using a 7000-series modified microliter syringe (Hamilton, Bonaduz, Switzerland).

For the test of PWN carrying beetles, the MaGal2 knockdown beetles were separately kept in ABM with PWN, as previously described. Late-stage pupae require approximately

2–3 days for eclosion, and six individuals were collected as samples to confirm expression levels of immune effector genes and PO activity at 4 days after eclosion. Three MaGal2-knockdown beetles, reared in sawdust, were collected as samples to confirm knockdown efficiency at 4 days after eclosion. GFP knockdown beetles served as controls. The 7-day-old adults were dissected and nematode loading was measured by counting individuals under a microscope.

Results

PWN loading and bacteria quantity in tracheae

Bacterial community dynamics in tracheae of *M. alternatus* following PWN loading was measured by comparing the quantity of cultivable bacteria by spread plate method and RT-qPCR relative quantity determination from PWN-loaded and nematode-free individuals. Results demonstrated that, after 100-fold dilution, both PWN-loaded and nematode-free tracheae had approximately 20 cultivatable CFUs (Fig. 1A) with no significant differences (Fig. 1B), even though there were massive amounts of cultivatable bacteria in ABM (Fig. S1C). Likewise, the relative quantity of all bacteria in tracheae using RT-qPCR showed no

significant differences (Fig. 1C), which is not surprising because the controls and treatments had ~20 CFUs each. These results indicated that the PWNs that loaded into beetles did not influence the quantity of bacteria in their vector's tracheae.

Because bacteria quantity in tracheae showed no changes upon nematode loading, we questioned whether it was because J_{IV} scarcely or rarely bound bacteria, or if the bacteria carried into the tracheae were somehow purged by the immune system in the vector's tracheae. To investigate the binding ability of J_{IV} to bacteria, we designed two experiments.

First, we added bacteria to the ABM and then checked if those bacteria could be observed in tracheae and transferred via nematodes. Because there were various species of associated symbiotic bacteria, we selected several representative bacteria species to perform the experiment. Based on the bacteria species isolated in the laboratory, we found that, among bacteria genera carried by PWNs, *Serratia* was detected throughout the invasion areas, and mostly with host pines and insect vectors, particularly in *M. alternatus* and *M. galloprovincialis* in particular (Nascimento *et al.*, 2015; Vicente *et al.*, 2016; Proenca *et al.*, 2017; Alves *et al.*, 2018). Hence, we chose *Serratia* and finally selected *S. marcescens*, which is an extensively studied, opportunistic pathogen that was recently reported to be associated with PWNs (Wei *et al.*, 2017a; Bai *et al.*, 2019). Even if there were abundant *S. marcescens* in the ABM, we did not observe a single *S. marcescens* colony on plates from

tracheae, which are easily observable because they turn red after 1 day (Fig. 2A). This result indicated that J_{IV} may not carry bacteria from the pupal chamber to the tracheae.

Second, we designed an experiment that let the nematodes freely creep out of the bacteria circle (Fig. S1A–B), and then tested for bacteria in their cuticle. To further verify this characteristic with J_{IV}, we selected some other nematode groups as controls. For these experiments, we chose propagative PWNs as a positive control, because propagative PWNs harbored symbiotic bacteria (Vicente *et al.*, 2016). Parasitic nematodes of pinewood, *Diplogasteroides asiaticus* (Fig. S1D), identified by 18srRNA sequencing and blast in NCBI (Fig. S1E), were chosen to explore the dominance of PWNs over other nematode species in pinewood and pupal chambers. The free-living nematode *C. elegans* was used as a control that represented nonparasitic nematodes. In addition, *S. marcescens* was selected as the candidate bacteria to potentially bind to nematodes because it is the dominant species in the bacterial community of host pines and vector insects. The results showed that no CFUs were observed in most J_{IV} group plates, but a significant amount of CFUs occurred in the other three groups' plates (Fig. 2B). To further verify if J_{IV} specifically could not bind *S. marcescens* but could possibly bind other bacteria, we performed this experiment with four other bacteria species, *Pseudomonas* sp., *Flexibacter aurantiacus*, *Pantoea* sp., and *Curtobacterium oceanosedimentum*, which were all isolated from the pupal chambers. These species have also been reported to be associated with PWD (Zhao *et al.*, 2014;

Nascimento *et al.*, 2015; Proenca *et al.*, 2017). Similarly, we observed that no CFUs were found in any plates of *Curtobacterium oceanosedimentum* and *Pseudomonas* sp., and more than half of the plates exhibited no CFUs for the other three bacterial species (Fig. 2C). Taken together, these results indicated that J_{IV} generally had a weak ability to bind bacteria in the pupal chamber.

Effects of S. marcescens isolated from the pupal chamber on M. alternatus beetle tracheae

As previous results suggested, PWNs do not carry large amounts of bacteria into the tracheae from the pupal chamber. Because the beetle can carry thousands of PWNs, we presumed that each nematode could bind at least 10 CFUs. Thus, to test the reaction of the *M. alternatus* beetle's immune system to foreign bacteria from an estimated 1000 nematodes, we chose *S. marcescens* as a representative bacterium and injected 10^4 CFUs of resuspended *S. marcescens* into the tracheae. The resulting survival curve demonstrated that beetles injected with bacteria died faster than members of the control group. Following injection of *S. marcescens* bacteria, all beetles carrying PWNs perished within 48 h. PWN-carrying controls injected with sterile water survived longer (Fig. 3A, *left*), whereas 95% of beetles injected with bacteria without PWNs gradually died after 48 h following infection, and died considerably faster compared with members of the control group that

were injected with sterile water (Fig. 3A, *right*). Clearly, these results indicated that *S. marcescens* infection facilitated the death of *M. alternatus* beetles and confirmed that the beetle immune system in the tracheae was unable to clear *S. marcescens*.

Because the bacterial infection triggered a high mortality rate, we questioned the strength of the immune responses upon bacterial infection in the presence of PWNs and if the immune balance was disrupted. To confirm if the activation of immune defenses in laboratory-reared beetles was consistent with previous field results (Zhou *et al.*, 2018), beetles that were reared for at least 10 generations in the laboratory were subjected to RT-qPCR and PO activity assays. To test the effect of *S. marcescens* on beetles carrying nematodes, 7-day-old *M. alternatus* beetles carrying PWNs that were reared in ABM were used, and beetles reared in medium without PWN were used as the control. We observed that, at 7 days post-eclosion, mRNA levels of PPO genes showed no significant changes in tracheae (Fig. S2A) or epidermises (Fig. S2B) when carrying PWNs. Consistent with mRNA results, the PO activity had no significant changes when carrying PWNs in tracheae (Fig. S2C) or epidermises (Fig. S2D). Similarly, several AMPs showed a relative decline in tracheae when carrying PWNs. Of these AMPs, cecropin and defensin showed a three-fold decrease, and attacin3 showed a two-fold decrease. Alternatively, lysozyme1 showed an approximately five-fold increase (Fig. S2E).

We subsequently performed RT-qPCR to check the expression level of immune effector genes 24 h post-*S. marcescens* infection, which coincided with the median lethal time in the presence or absence of nematodes. The immune genes showed a wide range of expression levels. In the presence of PWNs, *S. marcescens* infection significantly up-regulated expression levels of PPOs and some AMPs. PPO1 expression level exhibited a 3.4-fold increase and PPO2 had a 4.9-fold increase (Fig. 3B), whereas attacin2 showed a remarkable 21-fold increase (Fig. 3C) and lysozyme1 increased nearly three-fold (Fig. 3D). In contrast, *S. marcescens* infection decreased expression levels of several AMP genes, including defensin (Fig. 3E), cecropin (Fig. 3F), and attacin3 (Fig. S3A), which all decreased by more than 10-fold. In the absence of PWNs, among the immune effector genes examined in the tracheae, PPO1 was up-regulated, whereas PPO2 was down-regulated (Fig. S3B). Moreover, both attacin2 and lysozyme1 showed down-regulation, whereas attacin3, defensin1, and cecropin all showed up-regulation (Fig. S3C–G). Our results indicated that, regardless of whether the beetles carried PWNs, *S. marcescens* infection significantly disrupted the expression of effector genes in the immune system of the beetle; this led to a reduced survival rate. Consequently, *S. marcescens* infection did indeed devastate the immune system of vector beetles.

MaGal2, a PRR up-regulated in both the tracheae and epidermis

To determine whether the immune regulator participates in the regulation of immune evasion of PWN and weak melanization following PWN loading in vector beetles, we searched for recognition genes and compared our data with those published in a previous study (Zhou *et al.*, 2018). Zhou *et al.* (2018) demonstrated that PPO expression was up-regulated upon infection with the insect parasitic nematode *Howardula phyllotretae*; thus, in our study, we constructed heatmaps of the activity of recognition genes in beetles loaded with PWNs compared with nematode-free beetles, and of beetles infected by *H. phyllotretae* in both the tracheae and epidermis, because the epidermis is another tissue that contacts PWNs. The heatmaps showed that nine genes were up-regulated in the tracheae (Fig. S4A) and two genes were up-regulated in the epidermis (Fig. S4B); only MaGal2 was up-regulated in both tissues, which indicates that MaGal2 may be the key recognition gene involved in the dampened immune response.

The MaGal2 is a galectin family protein that contains a Gal-binding lectin domain, which has an affinity for *β*-galactosides. Based on the architecture predicted in swiss-model, MaGal2 is a proto-type galectin (Fig. S4C) that contains only one carbohydrate-recognition domain. The pairwise blast indicated that MaGal2 had close homology with galectin-4 of *Anoplophora glabripennis* (Fig. S4D). PCR and sequencing results of the full-length MaGal2 gene verified that there are three alternative splicing isoforms: isoform A, which contains all

1209 nucleotides of the ORF; isoform B, which contains 996 nucleotides and lacks the region from 763–975; and isoform C, which contains 882 nucleotides and lacks the region from 763–1089 (Fig. S4E). Additionally, western blot results indicated that the isoforms with higher expression were isoforms A and B (Fig. S4F).

To confirm the expression changes of MaGal2 after PWN inoculation, we performed RT-qPCR and western blot experiments. These results showed that the relative mRNA level of MaGal2 had nearly an eight-fold increase in the tracheae (Fig. 4A) and an approximately two-fold increase in the epidermis (Fig. 4B) after PWN inoculation. Additionally, the protein level of MaGal2 was consistent with the mRNA level and the band intensity of MaGal2 after PWN inoculation, and was higher in both tracheal (Fig. 4C) and epidermal (Fig. 4D) tissues compared with controls.

To confirm the up-regulated function of MaGal2, as a PRR gene involved in immune regulation, we synthesized recombinant MaGal2 protein and performed functional analysis before and after PWN inoculation to explore its possible association with the beetles' immune response relative to the nematodes' binding ability to bacteria. The recombinant MaGal2 encoded by isoform B with a carboxy-terminal His tag was expressed in a bacterial system. The soluble recombinant MaGal2 was purified and obtained by Ni-NTA superflow.

To confirm the binding properties of recombinant MaGal2 to microbes, we first performed an agglutination assay to examine the binding ability to the labeled Zymosan and *Staphylococcus aureus*. Results showed that recombinant MaGal2 could agglutinate Zymosan and *S. aureus* (Fig. 5A). Then, we examined the binding ability to bacteria isolated from pupal chambers, and results showed that all five bacterial species (*Serratia marcescens*, *Pseudomonas* sp., *Flexibacter aurantiacus*, *Pantoea* sp., and *Curtobacterium oceanosedimentum*) were agglutinated by recombinant MaGal2. These results indicated that MaGal2 could recognize bacteria and other microorganisms.

MaGal2 knockdown elevates melanization and reduces PWN loading

To further explore the exact role that MaGal2 plays in the regulation of immune response, we performed an RNAi experiment without PWN inoculation. The efficiency of the RNAi against MaGal2 was verified by RT-qPCR analysis of mRNA levels and western blot analysis of protein levels, which showed more than 80% down-regulation of MaGal2 compared with dsRNA of green fluorescent protein (dsGFP) treated newly eclosed adults in either the tracheae (Fig. 6A and C) or epidermis (Fig. 6B and D).

Following this initial experiment, we studied the changes of melanization after MaGal2 knockdown in the presence of PWN. The knockdown group was compared with the control group, which was injected with dsGFP. In the tracheae, the mRNA level of PPO1 and PPO2 more than doubled following dsMaGal2 injection (Fig. 6E); in the epidermis, it was almost doubled (Fig. 6F). Similarly, the PO activity of both tracheal (Fig. 6G) and epidermal (Fig. 6H) tissues were significantly elevated following MaGal2 knockdown. In contrast, the mRNA level of AMPs in tracheae was irregular, and attacin2, attacin3, cecropin, and defensin were all up-regulated, whereas lysozyme1 was down-regulated (Fig. S5). These results revealed that knockdown of MaGal2 elevated the level of melanization.

To analyze the effect of MaGal2 down-regulation on PWN loading, we performed an experiment to test PWN loading on dsMaGal2 knockdown beetles compared with controls. At 7 days post-eclosion, we observed that an average of 4153 PWNs were carried by each beetle injected with dsGFP, whereas only an average of 1571 PWNs were carried by each MaGal2 knockdown beetle (Fig. 6I). Thus, PWN loading was significantly decreased after MaGal2 RNAi, and this may be a result of up-regulation of melanization. Moreover, we detected the quantity of bacteria by RT-qPCR in RNAi-treated beetles in which melanization was up-regulated. The results demonstrated that there were no significant changes following MaGal2 knockdown (Fig. 6J), which indicated that the bacteria quantity in the tracheae was not influenced by melanization or other immune responses.

Discussion

Our study showed that differences in the tracheal bacteria quantity were negligible after PWN inoculation, which indicates that PWN loading did not influence the bacterial community in the tracheae of vector beetles. These findings further indicate that the vector beetles maintained a relatively stable quantity of symbiotic bacteria from the bacterial community in its tracheae, despite massive loading of J_{IV}. Insect pathogenic nematodes harbor symbiotic bacteria that help them successfully infect the host (Castillo *et al.*, 2011; Eleftherianos *et al.*, 2018). However, whether J_{IV} carry bacteria into vector tracheae remains unclear (Proenca *et al.*, 2017; Brivio & Mastore, 2018).

Our results demonstrated that J_{IV} carried far fewer bacteria on its surface, and J_{IV}'s ability to carry bacteria was much weaker relative to the propagative PWNs, pine parasitic nematode *D. asiaticus*, and free-living nematode *C. elegans*. These results demonstrate that the dispersing J_{IV} bind negligible amounts of bacteria while loading into the insect vectors' tracheae. Although we did not study the mechanistic reasons behind this phenomenon of binding few bacteria, we suspect that it may be related to the expression of some specific genes on the nematode's surface, as was reported in other nematode species (Darby, 2005; Bulgheresi *et al.*, 2011). Furthermore, surface sterilization did not influence bacteria

identified from *Steinernematidae* and *Heterorhabditidae* nematodes, which indicated that associated bacteria may have originated from inside the nematode (Gouge & Snyder, 2006). We noticed that the oral orifice of J_{IV} was degenerated and formed a closed body cavity, which may prevent the bacteria from flowing out from its intestine and presents another possible mechanism that limits bacterial transfers. The strategy of J_{IV} carrying few bacteria into the vector beetle is necessary to stabilize the bacterial community in the tracheae, which ensures protection of the vector beetle from destabilization of its microbial community following PWN loading and enables its dispersal to healthy trees.

Serratia marcescens is an opportunistic pathogen of insects and has been frequently identified in the insect gut and soils (Lee *et al.*, 2017; Wei *et al.*, 2017a; Gegner *et al.*, 2018). In addition, *S. marcescens* was also found to influence nematode pathogens and viral infections (Bai *et al.*, 2019; Wu *et al.*, 2019a). In fact, *Serratia* spp. were found in all habitats invaded by PWD (Zhao & Lin, 2005; Kwon *et al.*, 2010; Proenca *et al.*, 2010; Vicente *et al.*, 2011; Proenca *et al.*, 2014). Moreover, it was reported that propagative PWN incubated with *Serratia* strains showed deposits on the cuticle, whereas most *Serratia* strains exhibited high toxicity to PWNs (Paiva *et al.*, 2013; Vicente *et al.*, 2016). In this study, we observed only a few cultivable *Serratia* spp. in the tracheae of vector beetles carrying J_{IV}; however, injection of large amounts (10^4 CFUs) of *S. marcescens* facilitated the beetle's death.

We also observed that the controls injected with sterile water reduced the lifespan of beetles to some extent; therefore, we suspect that the blockages in the respiratory system may have contributed to asphyxiation and death of the beetle. Beetles injected with *S. marcescens* showed significantly higher mortality than the control group; these beetles indeed died of *S. marcescens* infection, as indicated by the tracheal tissues turning red. Therefore, the presence of *S. marcescens* in the tracheal system inoculated with J_{IV} resulted in higher, faster mortality of beetles compared with nematode-free beetles. This high mortality could help prevent the beetle from introducing PWNs to new host pine trees, because death occurs shortly after nematode loading and the beetles will consequently spread less PWD. Therefore, *S. marcescens* shows good potential as a biocontrol agent of PWNs, and this avenue for control should be further explored.

Melanization is a major innate immune response when tracheae are exposed to microorganisms (Ho *et al.*, 1982; Harris *et al.*, 1986; Tang *et al.*, 2008). A previous study demonstrated that PWN loading specifically activated the ROS and Toll pathways, and production of some AMPs, while it caused no significant changes in melanization, which is one of the earliest pathways activated by microbial infections in nematodes (Zhou *et al.*, 2018; Cooper *et al.*, 2019). Our study confirmed that melanization was not elevated after PWN inoculation in laboratory-reared beetles, but showed significant up-regulation upon *S. marcescens* injection. These findings demonstrated that, in an undisturbed beetle immune

system, melanization would not have been activated upon PWN loading and would result in a relatively balanced immune system. These results also indicate that J_{IV} PWNs transferred few bacteria into the beetle's tracheae; otherwise, the melanization would have been activated upon microorganism infection. In addition, as an invasive species, PWNs have distinct native vector beetle species worldwide, such as *M. carolinensis* in their native North America, *M. alternatus* and *M. saltuarius* in Asia, and *M. galloprovincialis* in Europe (Vicente *et al.*, 2013; Zhao *et al.*, 2014; Nascimento *et al.*, 2015). Each vector beetle species may have distinct symbiotic bacteria in their tracheal system (Alves *et al.*, 2016). As both host and symbionts coevolve and undergo coadaptation (Chapuis *et al.*, 2009; Florez *et al.*, 2015; Ledon-Rettig *et al.*, 2018), the phenomenon that J_{IV} carry almost no bacteria is possibly the result of coevolution between the vector beetle and PWNs to escape the host's immune response and achieve immune balance; this could be a defining characteristic that explains why PWNs spread so quickly worldwide.

Galectins serve as PRRs in innate immune responses (Vasta, 2009). However, the specific role of galectins in regulating innate immunity remains unknown in insects. Here, we observed that proto-type MaGal2 was up-regulated in both epidermal and tracheal tissues following PWN loading. Further results revealed that MaGal2 knockdown up-regulated the expression level of PPO genes and PO activities, which indicates that MaGal2 may be a negative regulator of melanization.

Previous studies have shown that symbiotic bacteria of the nematode *Steinernema carpocapsae* could suppress levels of host PO (Brivio *et al.*, 2018; Cooper *et al.*, 2019). *Manduca* PO was inhibited by *Photorhabdus* through a hydroxystilbene compound (Eleftherianos *et al.*, 2009). Unlike other nematodes, which depend on symbiotic bacteria to enhance their survival, PWNs utilize the vector's negative immune regulator MaGal2 to suppress their immune response, which is efficient and crafty. Moreover, PWN loading was significantly reduced following MaGal2 knockdown, which indicated that PWN loading is likely influenced by the beetle's immune response. However, bacteria loading was not influenced by MaGal2 knockdown, which indicated that bacteria loading does not normally occur in J_{IV}. In addition, galectins both mediate recognition and effector function in innate immunity, and also mediate developmental processes (Rao *et al.*, 2016; Zhang *et al.*, 2018a). However, MaGal2 may also have additional roles in *Monochamus* beetles, and should therefore be further studied.

Symbiotic microbes have been proven to play critical roles in invasive species, including PWNs (Wang *et al.*, 2012; Adams *et al.*, 2013; Wu *et al.*, 2013; Zhao *et al.*, 2014; Xu *et al.*, 2015; Zhou *et al.*, 2016; Cheng *et al.*, 2018a). However, our study revealed that, instead of recruiting symbiotic microbes, PWNs maintain a peaceful relationship by reducing bacteria, which may be the result of coevolution with its insect vector. The immune response mediator MaGal2 likely contributes to the stability of the symbiotic relationship between

PWNs and vector beetles, which is a strategy that helps ensure the PWN's fast and widespread invasion dynamics and ultimately causes devastating damage to pine forests worldwide. Breaking this immune balance may help disrupt the peaceful relationship that maintains the symbiosis (Fig. 7). Our study provides novel insight into the adaptive strategy of PWNs from the perspective of immune balance between PWNs and their vector beetles via a bacteria-free strategy.

Acknowledgements

This work was funded by the National Natural Science Foundation of China (31630013) and Frontier Science Key Project of the Chinese Academy of Sciences (QYZDJ-SSW-SMC024). We thank two anonymous reviewers for their constructive comments which improved the quality of the paper.

Disclosure

The authors declare no conflict of interest.

References

Adams, A.S., Aylward, F.O., Adams, S.M., Erbilgin, N., Aukema, B.H., Currie, C.R., *et al.* (2013) Mountain pine beetles colonizing historical and naive host trees are associated with a bacterial community highly enriched in genes contributing to terpene metabolism. *Applied and Environmental Microbiology*, 79, 3468–3475.

Alves, M., Pereira, A., Matos, P., Henriques, J., Vicente, C., Aikawa, T., *et al.* (2016) Bacterial community associated to the pine wilt disease insect vectors *Monochamus galloprovincialis* and *Monochamus alternatus*. *Scientific Reports*, 6, 23908.

Alves, M., Pereira, A., Vicente, C., Matos, P., Henriques, J., Lopes, H., *et al.* (2018) The role of bacteria in pine wilt disease: insights from microbiome analysis. *FEMS Microbiology Ecology*, 94(7), fiy077.

Backhed, F., Ley, R.E., Sonnenburg, J.L., Peterson, D.A. and Gordon, J.I. (2005) Host-bacterial mutualism in the human intestine. *Science*, 307, 1915–1920.

Bai, L., Wang, L., Vega-Rodriguez, J., Wang, G. and Wang, S. (2019) A gut symbiotic bacterium *Serratia marcescens* renders mosquito resistance to plasmodium infection through activation of mosquito immune responses. *Frontiers in Microbiology*, 10, 1580.

Belkaid, Y. and Harrison, O.J. (2017) Homeostatic immunity and the microbiota. *Immunity*, 46, 562–576.

Binda-Rossetti, S., Mastore, M., Protasoni, M. and Brivio, M.F. (2016) Effects of an entomopathogen nematode on the immune response of the insect pest red palm weevil: Focus on the host antimicrobial response. *Journal of Invertebrate Pathology*, 133, 110–119.

Brenner, S. (1974) The genetics of *Caenorhabditis elegans*. *Genetics*, 77, 71–94.

Brivio, M.F. and Mastore, M. (2018) Nematobacterial complexes and insect hosts: different weapons for the same war. *Insects*, 9, E117.

Brivio, M.F., Toscano, A., De Pasquale, S.M., De Lerma Barbaro, A., Giovannardi, S., Finzi, G. *et al.* (2018) Surface protein components from entomopathogenic nematodes and their symbiotic bacteria: effects on immune responses of the greater wax moth, *Galleria mellonella* (Lepidoptera: Pyralidae). *Pest Management Science*, doi: 10.1002/ps.4905.

Brubaker, S.W., Bonham, K.S., Zanoni, I. and Kagan, J.C. (2015) Innate immune pattern recognition: A cell biological perspective. *Annual Review of Immunology*, 33, 257–290.

Bulgheresi, S., Gruber-Vodicka, H.R., Heindl, N.R., Dirks, U., Kostadinova, M., Breiteneder, H. *et al.* (2011) Sequence variability of the pattern recognition receptor Mermaid mediates specificity of marine nematode symbioses. *The ISME Journal*, 5, 986–998.

Castillo, J.C., Reynolds, S.E. and Eleftherianos, I. (2011) Insect immune responses to nematode parasites. *Trends in Parasitology*, 27, 537–547.

Chapuis, E., Emelianoff, V., Paulmier, V., Le Brun, N., Pages, S., Sicard, M. *et al.* (2009) Manifold aspects of specificity in a nematode-bacterium mutualism. *Journal of Evolutionary Biology*, 22, 2104–2117.

Cheng, C., Wickham, J.D., Chen, L., Xu, D., Lu, M. and Sun, J.H. (2018a) Bacterial microbiota protect an invasive bark beetle from a pine defensive compound. *Microbiome*, 6, 132.

Cheng, Y., Lin, Z., Wang, J.M., Xing, L.S., Xiong, G.H. and Zou, Z. (2018b) CTL14, a recognition receptor induced in late stage larvae, modulates anti-fungal immunity in cotton bollworm *Helicoverpa armigera*. *Developmental and Comparative Immunology*, 84, 142–152.

Cooper, D., Wuebbolt, C., Heryanto, C. and Eleftherianos, I. (2019) The prophenoloxidase system in *Drosophila* participates in the anti-nematode immune response. *Molecular Immunology*, 109, 88–98.

Darby, C. (2005) Interactions with microbial pathogens. *Wormbook the Online Review of C Elegans Biology*, 6, 1–15.

Dawadi, B., Wang, X., Xiao, R., Muhammad, A., Hou, Y. and Shi, Z. (2018) PGRP-LB homolog acts as a negative modulator of immunity in maintaining the gut-microbe symbiosis of red palm weevil, *Rhynchophorus ferrugineus* Olivier. *Developmental and Comparative Immunology*, 86, 65–77.

Douglas, A.E. (2015) Multiorganismal insects: diversity and function of resident microorganisms. *Annual Review of Entomology*, 60, 17–34.

Douglas, A.E., Minto, L.B. and Wilkinson, T.L. (2001) Quantifying nutrient production by the microbial symbionts in an aphid. *The Journal of Experimental Biology*, 204, 349–358.

Eleftherianos, I., Waterfield, N.R., Bone, P., Boundy, S., Ffrench-Constant, R.H. and Reynolds, S.E. (2009) A single locus from the entomopathogenic bacterium *Photorhabdus luminescens* inhibits activated *Manduca sexta* phenoloxidase. *FEMS Microbiology Letters*, 293, 170–176.

Eleftherianos, I., Yadav, S., Kenney, E., Cooper, D., Ozakman, Y. and Patrnogic, J. (2018) Role of endosymbionts in insect-parasitic nematode interactions. *Trends in Parasitology*, 34, 430–444.

Fielding, N.J. and Evans, H.F. (1996) The pine wood nematode *Bursaphelenchus xylophilus* (Steiner and Buhrer) Nickle (= *B. lignicolus* Mamiya and Kiyohara): an assessment of the current position. *Forestry: An International Journal of Forest Research*, 69, 35–46.

Florez, L.V., Biedermann, P.H.W., Engl, T. and Kaltenpoth, M. (2015) Defensive symbioses of animals with prokaryotic and eukaryotic microorganisms. *Natural Product Reports*, 32, 904–936.

Gegner, T., Carrau, T., Vilcinskas, A. and Lee, K.Z. (2018) The infection of *Harmonia axyridis* by a parasitic nematode is mediated by entomopathogenic bacteria and triggers sex-specific host immune responses. *Scientific Reports*, 8, 15938.

Gouge, D.H. and Snyder, J.L. (2006) Temporal association of entomopathogenic nematodes (Rhabditida: *Steinernematidae* and *Heterorhabditidae*) and bacteria. *Journal of Invertebrate Pathology*, 91, 147–157.

Harris, K.L., Christensen, B.M. and Miranpuri, G.S. (1986) Comparative studies on the melanization response of male and female mosquitoes against microfilariae. *Developmental and Comparative Immunology*, 10, 305–310.

Ho, B.C., Yap, E.H. and Singh, M. (1982) Melanization and encapsulation in *Aedes aegypti* and *Aedes togoi* in response to parasitization by a filarioid nematode (*Breinlia booliati*). *Parasitology*, 85 (Pt 3), 567–575.

Ji, D. and Kim, Y. (2004) An entomopathogenic bacterium, *Xenorhabdus nematophila*, inhibits the expression of an antibacterial peptide, cecropin, of the beet armyworm, *Spodoptera exigua*. *Journal of Insect Physiology*, 50, 489–496.

Kurata, S. (2010) Fly immunity: recognition of pathogens and induction of immune responses. *Advances in Experimental Medicine and Biology*, 708, 205–217.

Kwon, H.R., Choi, G.J., Choi, Y.H., Jang, K.S., Sung, N.D., Kang, M.S., *et al.* (2010) Suppression of pine wilt disease by an antibacterial agent, oxolinic acid. *Pest Management Science*, 66, 634–639.

Ledon-Rettig, C.C., Moczek, A.P. and Ragsdale, E.J. (2018) *Diplogastrellus* nematodes are sexually transmitted mutualists that alter the bacterial and fungal communities of their beetle host. *Proceedings of the National Academy of Sciences USA*, 115, 10696–10701.

Lee, D.J., Lee, J.B., Jang, H.A., Ferrandon, D. and Lee, B.L. (2017) An antimicrobial protein of the Riptortus pedestris salivary gland was cleaved by a virulence factor of *Serratia marcescens*. *Developmental and Comparative Immunology*, 67, 427–433.

Lu, M., Hulcr, J. and Sun, J.H. (2016) The role of symbiotic microbes in insect invasions. *Annual Review of Ecology, Evolution, and Systematics*, 47, 487–505.

Morales-Jimenez, J., Zuniga, G., Villa-Tanaca, L. and Hernandez-Rodriguez, C. (2009) Bacterial community and nitrogen fixation in the red turpentine beetle, *Dendroctonus valens* LeConte (Coleoptera: Curculionidae: Scolytinae). *Microbial Ecology*, 58, 879–891.

Nakanishi, K., Hoshino, M., Nakai, M. and Kunimi, Y. (2008) Novel RNA sequences associated with late male killing in *Homona magnanima*. *Proceedings. Biological Sciences*, 275, 1249–1254.

Nascimento, F.X., Hasegawa, K., Mota, M. and Vicente, C.S. (2015) Bacterial role in pine wilt disease development–review and future perspectives. *Environmental Microbiology Reports*, 7, 51–63.

Paiva, G., Proença, D.N., Francisco, R., Verissimo, P., Santos, S.S., Fonseca, L., *et al.* (2013) Nematicidal bacteria associated to pinewood nematode produce extracellular proteases. *PLoS ONE*, 8, e79705.

Park, Y., Kim, Y., Tunaz, H. and Stanley, D.W. (2004) An entomopathogenic bacterium, *Xenorhabdus nematophila*, inhibits hemocytic phospholipase A2 (PLA2) in tobacco hornworms *Manduca sexta*. *Journal of Invertebrate Pathology*, 86, 65–71.

Proenca, D.N., Fonseca, L., Powers, T.O., Abrantes, I.M. and Morais, P.V. (2014) Diversity of bacteria carried by pinewood nematode in USA and phylogenetic comparison with isolates from other countries. *PLoS ONE*, 9, e105190.

Proenca, D.N., Francisco, R., Santos, C.V., Lopes, A., Fonseca, L., Abrantes, I.M., *et al.* (2010) Diversity of bacteria associated with *Bursaphelenchus xylophilus* and other nematodes isolated from *Pinus pinaster* trees with pine wilt disease. *PLoS ONE*, 5, e15191.

Proenca, D.N., Grass, G. and Morais, P.V. (2017) Understanding pine wilt disease: roles of the pine endophytic bacteria and of the bacteria carried by the disease-causing pinewood nematode. *Microbiologyopen*, 6, e415.

Rao, X.J., Wu, P., Shahzad, T., Liu, S., Chen, L., Yang, Y.F., *et al.* (2016) Characterization of a dual-CRD galectin in the silkworm *Bombyx mori*. *Developmental and Comparative Immunology*, 60, 149–159.

Sadekuzzaman, M., Park, Y., Lee, S., Kim, K., Jung, J.K. and Kim, Y. (2017) An entomopathogenic bacterium, *Xenorhabdus hominickii* ANU101, produces oxindole and suppresses host insect immune response by inhibiting eicosanoid biosynthesis. *Journal of Invertebrate Pathology*, 145, 13–22.

Tang, H., Kambris, Z., Lemaitre, B. and Hashimoto, C. (2008) A serpin that regulates immune melanization in the respiratory system of *Drosophila*. *Developmental Cell*, 15, 617–626.

Tanji, T. and Ip, Y.T. (2005) Regulators of the Toll and Imd pathways in the *Drosophila* innate immune response. *Trends in Immunology*, 26, 193–198.

Vasta, G.R. (2009) Roles of galectins in infection. *Nature Reviews. Microbiology*, 7, 424–438.

Vicente, C.S., Nascimento, F., Espada, M., Mota, M. and Oliveira, S. (2011) Bacteria associated with the pinewood nematode *Bursaphelenchus xylophilus* collected in Portugal. *Antonie Van Leeuwenhoek*, 100, 477–481.

Vicente, C.S., Nascimento, F.X., Barbosa, P., Ke, H.M., Tsai, I.J., Hirao, T., *et al.* (2016) Evidence for an opportunistic and endophytic lifestyle of the *Bursaphelenchus xylophilus*-associated bacteria *Serratia marcescens* PWN146 isolated from wilting *Pinus pinaster*. *Microbial Ecology*, 72, 669–681.

Vicente, C.S., Nascimento, F.X., Espada, M., Barbosa, P., Hasegawa, K., Mota, M., *et al.* (2013) Characterization of bacterial communities associated with the pine sawyer beetle *Monochamus galloprovincialis*, the insect vector of the pinewood nematode *Bursaphelenchus xylophilus*. *FEMS Microbiology Letters*, 347, 130–139.

Volovych, O., Lin, Z., Du, J., Jiang, H. and Zou, Z. (2019) Identification and temporal expression profiles of cuticular proteins in the endoparasitoid wasp, *Microplitis mediator*. *Insect Science*, doi: 10.1111/1744-7917.12711.

Wang, B., Lu, M., Cheng, C., Salcedo, C. and Sun, J.H. (2012) Saccharide-mediated antagonistic effects of bark beetle fungal associates on larvae. *Biology Letters*, 9, 20120787.

Wang, J.M., Cheng, Y., Shi, Z.K., Li, X.F., Xing, L.S., Jiang, H., *et al.* (2019) Aedes aegypti HPX8C modulates immune responses against viral infection. *PLoS Neglected Tropical Diseases*, 13, e0007287.

Wei, G., Lai, Y., Wang, G., Chen, H., Li, F. and Wang, S. (2017a) Insect pathogenic fungus interacts with the gut microbiota to accelerate mosquito mortality. *Proceedings of the National Academy of Sciences USA*, 114, 5994–5999.

Wei, G., Lai, Y., Wang, G., Chen, H. and Wang, S. (2017b) Insect pathogenic fungus interacts with the gut microbiota to accelerate mosquito mortality. *Proceedings of the National Academy of Sciences USA*, 114, 5994–5999.

Wu, P., Sun, P., Nie, K., Zhu, Y., Shi, M., Xiao, C., *et al.* (2019a) A gut commensal bacterium promotes mosquito permissiveness to arboviruses. *Cell Host Microbe*, 25, 101–112 e5.

Wu, X.Q., Yuan, W.M., Tian, X.J., Fan, B., Fang, X., Ye, J.R. *et al.* (2013) Specific and functional diversity of endophytic bacteria from pine wood nematode *Bursaphelenchus Xylophilus* with different virulence. *International Journal of Biological Sciences*, 9, 33–44.

Wu, Y., Wickham, J. D., Zhao, L. and Sun, J.H. (2019b) CO_2 drives the pine wood nematode off its insect vector. *Current Biology*, 29, R619–R620.

Xu, L., Lou, Q., Cheng, C., Lu, M. and Sun, J.H. (2015) Gut-associated bacteria of *Dendroctonus valens* and their involvement in verbenone production. *Microbial Ecology*, 70, 1012–1023.

Yu, X.Q. and Kanost, M.R. (2000) Immulectin-2, a lipopolysaccharide-specific lectin from an insect, *Manduca sexta*, is induced in response to gram-negative bacteria. *The Journal of Biological Chemistry*, 275, 37373–37381.

Yuan, C., Xing, L., Wang, M., Wang, X., Yin, M., Wang, Q., *et al.* (2017) Inhibition of melanization by serpin-5 and serpin-9 promotes baculovirus infection in cotton bollworm *Helicoverpa armigera*. *PLoS Pathogens*, 13, e1006645.

Zhang, L.L., Hu, X.H., Wu, S.Q., Batool, K., Chowdhury, M., Lin, Y., *et al.* (2018a) *Aedes aegypti* galectin competes with Cry11Aa for binding to ALP1 to modulate cry toxicity. *Journal of Agricultural and Food Chemistry*, 66, 13435–13443.

Zhang, X., Sun, Z., Zhang, X., Zhang, M. and Li, S. (2018b) Hemolymph microbiomes of three aquatic invertebrates as revealed by a new cell extraction method. *Applied and Environmental Microbiology*, 84, e02824-17.

Zhao, B.G. and Lin, F. (2005) Mutualistic symbiosis between *Bursaphelenchus xylophilus* and bacteria of the genus *Pseudomonas*. *Forest Pathology*, 35, 339–345.

Zhao, L., Mota, M., Vieira, P., Butcher, R.A. and Sun, J.H. (2014) Interspecific communication between pinewood nematode, its insect vector, and associated microbes. *Trends in Parasitology*, 30, 299–308.

Zhao, L., Zhang, S., Wei, W., Hao, H., Zhang, B., Butcher, R.A., *et al.* (2013) Chemical signals synchronize the life cycles of a plant-parasitic nematode and its vector beetle. *Current Biology*, 23, 2038–2043.

Zhao, L., Wei, W., Kang, L. and Sun, J. (2007) Chemotaxis of the pinewood nematode, *Bursaphelenchus xylophilus*, to volatiles associated with host pine, *Pinus massoniana*, and its vector *Monochamus alternatus*. *Journal of Chemical Ecology*, 33, 1207–1216.

Zhou, F., Lou, Q., Wang, B., Xu, L., Cheng, C., Lu, M., *et al.* (2016) Altered carbohydrates allocation by associated bacteria–fungi interactions in a bark beetle-microbe symbiosis. *Scientific Reports*, 6, 20135.

Zhou, J., Zhao, L., Yu, H.Y., Wang, Y.H., Zhang, W., Hu, S.N., *et al.* (2018) Immune tolerance of vector beetle to its partner plant parasitic nematode modulated by its insect parasitic nematode. *FASEB Journal*, 32, 4862–4877.

Manuscript received March 19, 2020

Final version received April 24, 2020

Accepted May 4, 2020

Figure legend

Fig. 1 PWN loading did not significantly change the quantity of bacteria in tracheae. (A) Load of cultivable bacteria in tracheae from nematode-free controls (Tr-CK) and nematode loaded (Tr-PWN) vector beetles. Bacterial load was determined by plating the homogenate of tracheal tissue in one beetle with 1 : 100 dilution on TSA plates. Representative images are shown. (B) Number of CFU on each plate were counted and analyzed, and (C) relative quantification was determined by 16s rRNA gene-based RT-qPCR analysis. Tr, tracheae; CK (control), nematode-free tracheae; PWN, PWN loaded tracheae. Data were normalized to

controls. At least three biological replicates were conducted. Error bars indicate SD. ns, no significant difference determined by the Student's *t*-test at $P > 0.05$.

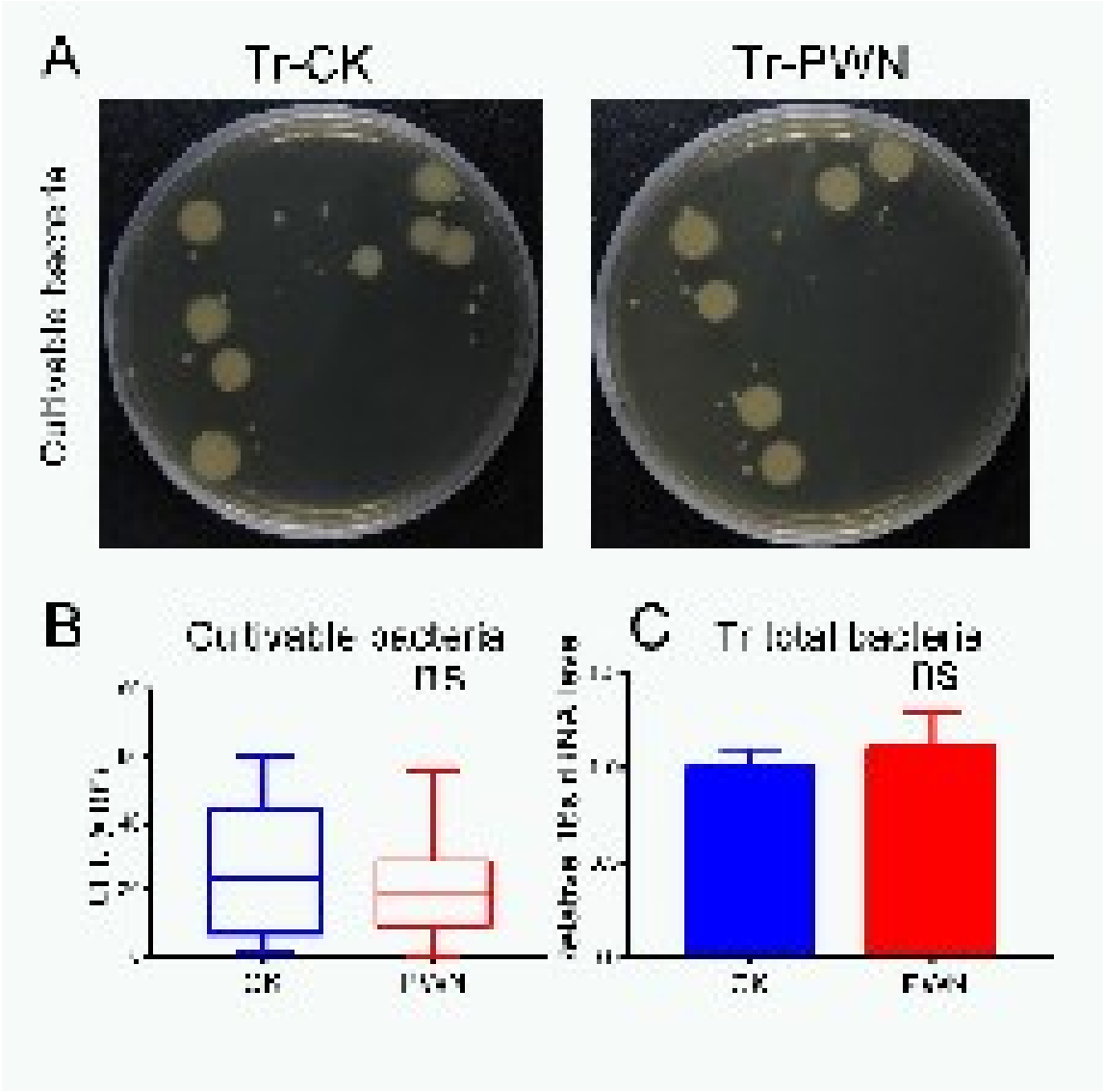

Fig. 2 J_{IV} scarcely bound bacteria on the surface (A) Cultivable bacteria from artificial barley medium (left) and PWN loaded *Monochamus* beetle tracheae (right). Bacterial load from *S. marcescens* co-cultured artificial barley medium was determined by plating the homogenate

of 0.1 g medium with 1 : 10000 dilution on TSA plates. PWN loaded *Monochamus* beetles were reared in *S. marcescens* co-cultured artificial barley medium. Bacterial load was determined by plating the homogenate of tracheae with 1 : 100 dilution on TSA plates. Plates were cultured for 3 days. Representative images are shown. (B) *S. marcescens* quantity carried by four nematode species, J_{IV}, propagative PWN, *D. asiaticus*, *C.elegans*. (C) Bacterial quantity carried by J_{IV} using four species isolated from wild pupal chamber. Bacterial quantity carried by nematode was determined by binding analysis of nematode. At least five biological replicates were conducted. Error bars indicate SD. **, significant differences as determined by Student's *t*-test at $P < 0.01$.

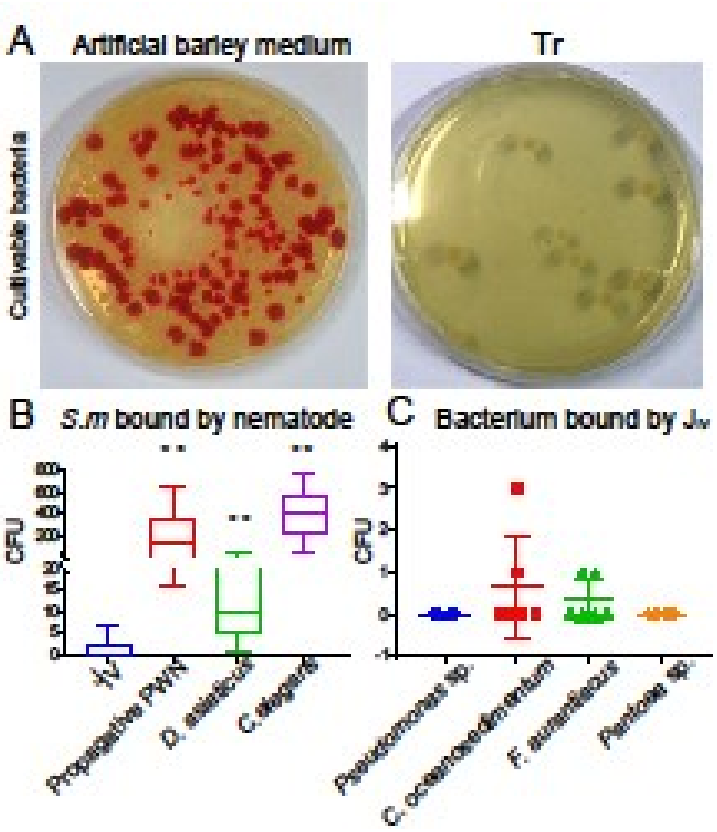

Fig. 3 Bacteria *S. marcescens* isolated from pupal chamber are unfavorable to *Ma* beetle and disrupt the immune balance in tracheae. (A) Survival curve of *Monochamus alternatus* (*n* = 10) infected (S.m) or uninfected controls (CK) by *S. marcescens*. 10^4 CFU bacteria *S. marcescens* were injected into tracheae and cultured in the presence of PWN in ABM or in the absence of PWN, injection with sterile water served as control. Injections were conducted carefully and tracheae showed no wounds. Log-rank (Mantel Cox test) was used to calculate statistical significance. (B–F) Relative quantity of mRNA expression level of PPO (B), Attaincin2 (C), Lysozyme1 (D), Defensin (E), Cecropin (F), genes in tracheae 24 hours post infection (hpi) in the presence of PWN. Tr, tracheae; CK-PWN, tracheae inject sterile water in the presence of PWN; Sm-PWN, tracheae injected with *S. marcescens* in the presence of PWN. Data were normalized to the expression level of CK-PWN. Three biological replicates were conducted. Error bars indicate SD. **, significant difference determined by the Student's *t*-test at $P < 0.01$.

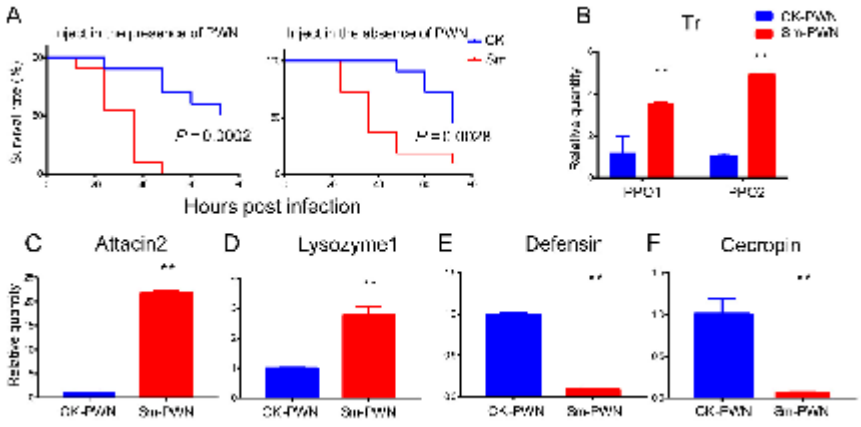

Fig. 4 MaGal2, a pattern-recognition receptor (PRR) gene, was up-regulated in both tracheae and epidermis. (A and B) relative quantity of MaGal2 mRNA expression level in tracheae (A) and epidermis (B). (C and D) Immunoblot analysis of MaGal2 in tracheae (C) and epideimis (D). α-Tubulin were used as loading controls. Tr, tracheae; Ep, epidermis; CK, tracheae or epidermis of beetle not carrying PWN; PWN, tracheae or epidermis of beetle carrying PWN. Data were normalized to the expression level of CK. Three biological replicates were conducted. Error bars indicate SD. **, significant difference determined by the Student's *t*-test at $P < 0.01$.

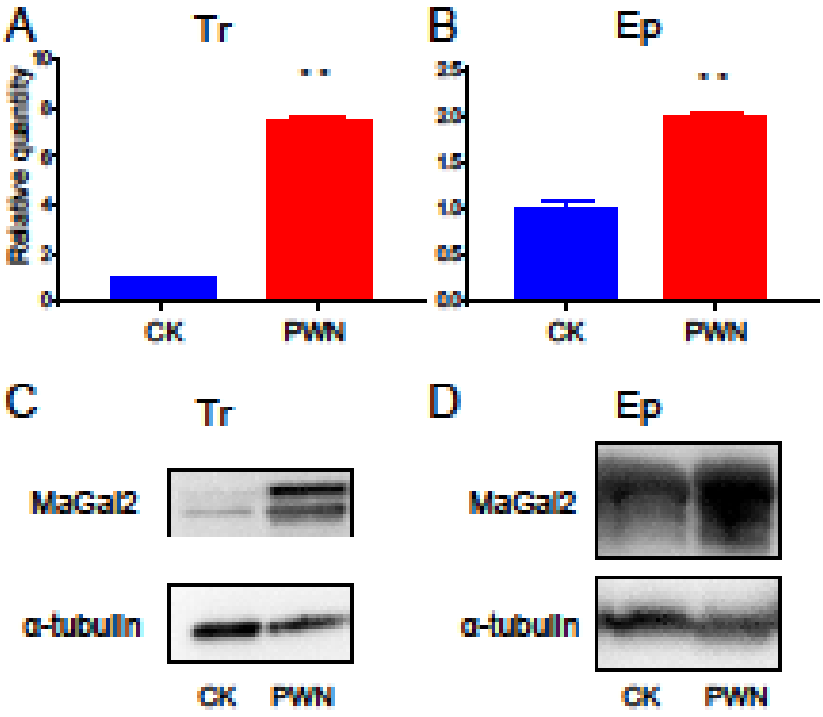

Fig. 5 rMaGal2 function in agglutination. (A and B) The agglutination assay testing interaction of rGalectin2 with zymosan, *S. aureus* (A) and five bacteria species isolated from pupal chamber (B). Purified rGalectin2 samples were incubated with labeled zymosan, *S. aureus* and five other bacteria species for 3 hours. BSA was set as negative control. Arrows indicate the aggregates. Representative image are shown.

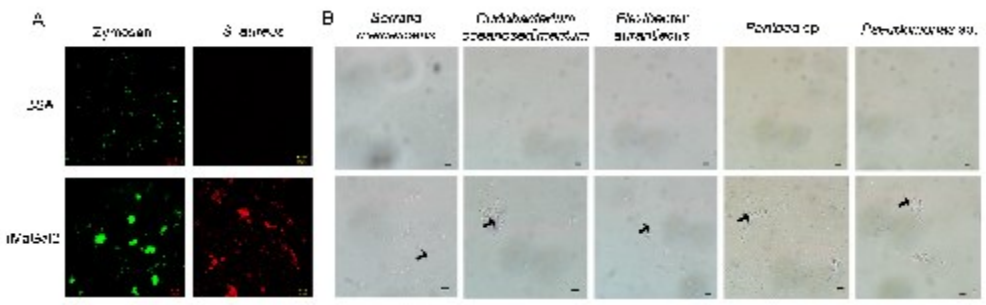

Fig. 6 MaGal2 knockdown up-regulates melanization and reduces PWN loading. (A and B) Relative quantity of mRNA expression level of MaGal2 in tracheae (A) and epidermis (B) upon MaGal2 knockdown. (C and D) Immunoblot analysis of MaGal2 in tracheae (C) and epidermis (D) upon MaGal2 knockdown. α-Tubulin was used as the loading control. (E and F) Relative quantity of MaGal2 depleted mRNA expression level of PPO in tracheae (E) and epidermis (F). (G and H) PO activity of MaGal2 depleted adult carrying PWN in tracheae (G) and epidermis (H). (I) PWN loading upon MaGal2 knockdown. (J) Relative quantity of bacteria in tracheae upon MaGal2 knockdown. Tr, tracheae; Ep, epidermis; iGFP, GFP-depleted adult; iMaGal2, MaGal2-depleted adult; iGFP-PWN, GFP-depleted adult carrying PWN; iMaGal2-PWN, MaGal2-depleted adult carrying PWN. Data were normalized

to the expression level of iGFP or iGFP-PWN. Three biological replicates were conducted. Error bars indicate SD. **, significant difference determined by the Student's *t*-test at $P < 0.01$. *, significant difference determined by the Student's *t*-test at $P < 0.05$. ns, no significant difference.

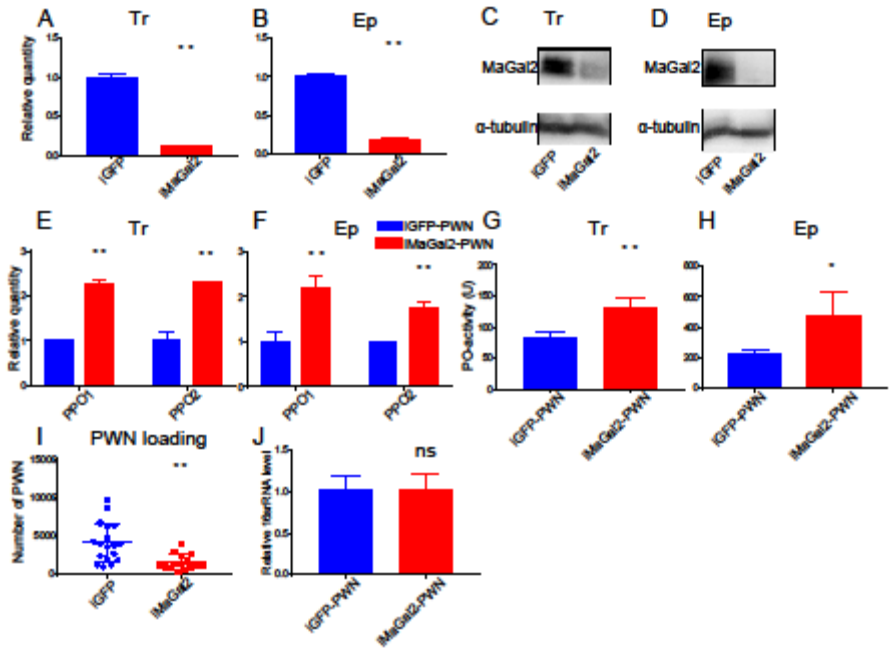

Fig. 7 Proposed model of PWN immune evasion strategy. J_{IV} enter the tracheal system of their vector beetle while taking in negligible amounts of bacteria, even if nematodes were surrounded by a variety of abundant bacteria in the pupal chamber, and thus achieve a peaceful relationship with its vector beetle to preserve the symbiosis. Furthermore, with the loading of PWN, the pattern-recognition receptor MaGal2 was elevated. However, MaGal2 agglutinate few bacteria as J_{IV} carry negligible bacteria into the tracheae. Then, as a negative

regulator of melanization, MaGal2 suppressed the PO activity and contributed to the maintenance of immune balance in tracheae.